Calcium Waves along the Cleavage Furrows in Cleavage-Stage *Xenopus* Embryos and Its Inhibition by Heparin

Akira Muto,*‡¶ Shoen Kume,‡¶ Takafumi Inoue,‡ Hideyuki Okano,‡§‖ and Katsuhiko Mikoshiba*‡¶

*Molecular Neurobiology Laboratory, Tsukuba Life Science Center, Institute of Physical and Chemical Research (RIKEN), Tsukuba-City, Ibaraki-Prefecture 305, Japan; ‡Department of Molecular Neurobiology, Institute of Medical Science, University of Tokyo, Minato-ku, Tokyo 108, Japan; §Department of Molecular Neurobiology, Institute of Medical Sciences and Center for TARA, University of Tsukuba, Tsukuba 305, Japan; ‖Core Research for Evolutional Science and Technology, Japan Science and Technology Corporation, Shinagawa-ku, Tokyo 140, Japan; and ¶Calciosignal Net Project, Exploratory Research for Advanced Technology, Japan Science and Technology Corporation, Meguro-ku, Tokyo 153, Japan

Abstract. Calcium signaling is known to be associated with cytokinesis; however, the detailed spatio-temporal pattern of calcium dynamics has remained unclear. We have studied changes of intracellular free calcium in cleavage-stage *Xenopus* embryos using fluorescent calcium indicator dyes, mainly Calcium Green-1. Cleavage formation was followed by calcium transients that localized to cleavage furrows and propagated along the furrows as calcium waves. The calcium transients at the cleavage furrows were observed at each cleavage furrow at least until blastula stage. The velocity of the calcium waves at the first cleavage furrow was ~3 μm/s, which was much slower than that associated with fertilization/egg activation. These calcium waves traveled only along the cleavage furrows and not in the direction orthogonal to the furrows. These observations imply that there exists an intracellular calcium–releasing activity specifically associated with cleavage furrows. The calcium waves occurred in the absence of extracellular calcium and were inhibited in embryos injected with heparin, an inositol 1,4,5-trisphosphate ($InsP_3$) receptor antagonist. These results suggest that $InsP_3$ receptor–mediated calcium mobilization plays an essential role in calcium wave formation at the cleavage furrows.

INTRACELLULAR calcium ions are thought to participate in the regulation of several aspects of cell division (for review see Hepler, 1994). Calcium transients have been observed at pronuclear migration and fusion, nuclear envelope breakdown, anaphase onset, and cytokinesis in the first cell cycle of sea urchin embryos (Ciapa et al., 1994; Poenie et al., 1985) or before nuclear envelope breakdown in the first cell cycle of mouse eggs (Tombes et al., 1992). As the contractile ring is composed of an actomyosin system (Cao and Wang, 1990; Mittal et al., 1987), it has been proposed that calcium signaling is directly involved in cytokinesis. However, while some groups have observed calcium transients at cytokinesis (Ciapa et al., 1994; Poenie et al., 1985), some other studies on calcium changes during the cell division cycle have not provided evidence for calcium increase at cytokinesis. Although periodic changes in intracellular calcium concentration were observed to be associated with cleavage cycles in medaka embryos (Yoshimoto et al., 1985) and in *Xenopus* embryos (Grandin and Charbonneau, 1991), cytokinesis started at the trough of the calcium oscillation. The timing of the peak of the periodic calcium oscillation was shown to correspond with metaphase in *Xenopus* embryos (Kubota et al., 1993). Recently, the spatio-temporal pattern of calcium transients at cytokinesis has been reported in medaka fish embryos (Fluck et al., 1991) and zebra fish embryos (Chang and Meng, 1995). Two types of calcium waves at cytokinesis were described (Fluck et al., 1991): one seemed to be associated with the extension of the cleavage furrow, and the other with subsequent apposition of the newly generated adjacent blastomeres. While they did not observe calcium transients preceding the formation of the cleavage furrows in medaka fish embryos, calcium transients were shown to occur at the site where the cleavage furrow would form in zebra fish embryos (Chang and Meng, 1995).

The regulation of intracellular calcium concentration has been shown to be essential for cell cycle progression in several previous studies. Chelation of intracellular calcium ions has been shown to retard cell division in *Xenopus* embryos (Snow and Nuccitelli, 1993). Both anti-phosphatidylinositol bisphosphate antibody, which blocks hydrolysis

Address all correspondence to Akira Muto, Calciosignal Net Project, Exploratory Research for Advanced Technology (ERATO), Japan Science and Technology Corporation (JST), 2-9-3 Shimo-meguro, Meguro-ku, Tokyo 153, Japan. Tel.: (81) 3-3492-0231. Fax: (81) 3-3492-0233. e-mail: muto@ims.u-tokyo.ac.jp.

A. Muto and S. Kume's present address is Calciosignal Net Project, ERATO, JST, 2-9-3 Shimo-meguro, Meguro-ku, Tokyo 153, Japan.

of phosphatidylinositol bisphosphate, and heparin, an inhibitor of the inositol 1,4,5-trisphosphate ($InsP_3$)[1] receptor, inhibited cell cycle progression in *Xenopus* embryos (Han et al., 1992). In sea urchin eggs, changes in $InsP_3$ mass were demonstrated to be associated with calcium transients during the first embryonic cell cycle (Ciapa et al., 1994). Calcium transients observed during cell cycle progression were shown to be inhibited by heparin (Chang and Meng, 1995; Ciapa et al., 1994). These results suggested that polyphosphoinositide turnover and calcium mobilization from $InsP_3$-sensitive calcium stores are involved in cell cycle progression.

Since previous studies have not characterized the spatio-temporal pattern of calcium dynamics during cell division cycle (Grandin and Charbonneau, 1991; Keating et al., 1994; Kubota et al., 1993), it has remained unclear how free calcium concentrations change and how they are associated with events in the cell division cycle of *Xenopus* embryos. Here we report the calcium dynamics at early cleavage-stage in *Xenopus* embryos using calcium-sensitive fluorescent dyes, mainly using Calcium Green-1. Calcium waves were observed along the cleavage furrows after cleavage furrow formation. Calcium mobilization occurred in the absence of extracellular calcium and was blocked by heparin. These results suggest that $InsP_3$ receptor–mediated calcium mobilization occurs along the cleavage furrows. Furthermore, we have demonstrated that the calcium waves that occur along the cleavage furrows can be distinguished from the sinusoidal calcium oscillations that occur at the same frequency as that of the cell cycle.

Materials and Methods

Microinjection and Treatments of Xenopus laevis Embryos

Adult males and females of *Xenopus laevis* were purchased from Hamamatsu Seibutsu Kyozai (Hamamatsu, Japan), Kamogawa Seibutsu Kyozai (Chiba, Japan), or Alps Kagaku Boeki (Shinagawa, Japan). *Xenopus laevis* females were injected with 750 U of human chorionic gonadotropin (Sigma Chemical Co., St. Louis, MO). On the following day, unfertilized ovulated eggs were stripped from the animals into modified Barth's saline (88 mM NaCl, 1.0 mM KCl, 2.4 mM $NaHCO_3$, 15 mM Hepes, pH 7.6, 0.3 mM $Ca(NO_3)_2$, 0.41 mM $CaCl_2$, 0.82 mM $MgSO_4$, 50 U/ml sodium penicillin, and 50 μg/ml streptomycin sulfate) and were fertilized in vitro. The jelly layer was removed with 2 or 3% cystein, pH 7.8, in 1× or 0.1× Steinberg's solution (1×: 60 mM NaCl, 0.67 mM KCl, 0.34 mM $Ca(NO_3)_2$, 0.84 mM $MgSO_4$, 10 mM Hepes). Dejellied eggs were transferred into 1× Steinberg's solution (pH 7.4) containing 5% Ficoll 400 (Pharmacia Fine Chemicals, Piscataway, NJ) and injected with 20 nl of 0.375 or 0.5 mM Calcium Green-1 (Molecular Probes, Inc., Eugene, OR), or a mixture of 0.375 mM Calcium Green-1–dextran (mol wt = 10,000) (Molecular Probes, Inc.) and 1 mM rhodamine B-dextran (mol wt = 10,000) (Molecular Probes, Inc.) in an injection buffer (88 mM NaCl, 1 mM KCl, 15 mM Tris-HCl, pH 7.5). The volume of the injected solution was estimated by measuring the diameter of droplets injected into the air. Eggs were injected on the animal side at four equally spaced points with 5 nl of the injection solution (total of 20 nl) to assure uniform diffusion of injected material until measurement. Either heparin (mol wt = 3,500; Sigma Chemical Co.) or de-N-sulfated heparin (Sigma Chemical Co.) was coinjected with Calcium Green-1 when used. The eggs were kept at 17°C to slow down cell cycle progression. When the first cleavage furrow appeared at the animal pole, the eggs were washed with the same medium used in the measurements, and the dye fluorescence was monitored by confocal microscopy. The experiments were carried out in 0.02–1× Steinberg's solution. *Xenopus* eggs usually developed normally to tadpoles in this condition.

Confocal Microscopy

Images were acquired on a confocal laser microscope system, (MRC-500; Bio-Rad Laboratories, Hercules, CA) adapted to an inverted microscope (IMT-2; Olympus Corp., Tokyo, Japan) (objective lens: Plan 4/0.13 NA (×4); Nikon Inc., Tokyo, Japan) using CoMOS and TCSM software packages (Bio-Rad Microscience). The focus was adjusted to the egg surface of the vegetal pole, and the confocal aperture was set to be fully open to maximize the collection of the fluorescence. All measurements were carried out at room temperature (24–27°C). Consecutively acquired 5–10 images were averaged on line by Kalman algorithm, except for the images in Fig. 3. The images in Fig. 3 were obtained by averaging three successive images taken by single scans at an interval of 10 s. The resulting images were further median-filtered to reduce noise off line. The off-line image processing was carried out on Macintosh computers using a public domain NIH Image program (written by Wayne Rasband at the United States National Institutes of Health and available from the Internet by anonymous FTP from zippy.nimh.nih.gov or on floppy disk from NTIS, 5285 Port Royal Rd., Springfield, VA 22161, part PB93-504868). To show the changes in Calcium Green-1 fluorescence intensity, the fluorescent images at indicated times (min: designated as ') were divided pixel-by-pixel with an image taken before calcium transients had occurred (the image at 0'). This sometimes brought about an artificial increase of ratio at the edge of blastomere as a result of slight morphological changes, but the nonuniformity of the fluorescence over the entire egg was effectively eliminated.

Calcium Release from Microsomes of Xenopus Eggs/Embryos

Microsomes of *Xenopus* embryos were prepared as described by Parys et al. (1992) with some modifications. *Xenopus* embryos at early cleavage stage (1–8-cell stages) were dejellied and homogenized in 4 vol of ice-cold buffer containing 50 mM of Tris-HCl, pH 7.25, 250 mM sucrose, 1 mM EGTA, 1 mM DTT, 0.1 mM PMSF, 10 μM leupeptin, and 1 μM pepstatin A by four strokes in a 20-ml glass-Teflon homogenizer. The homogenate was centrifuged at 4,500 *g* for 15 min. The supernatant was centrifuged at 160,000 *g* for 35 min at 2°C. The pellet was resuspended in an ice-cold buffer containing 20 mM Tris-HCl, pH 7.25, 300 mM sucrose, 1 mM EGTA, 1 mM DTT, 0.1 mM PMSF, 10 μM leupeptin, and 1 μM pepstatin A, frozen in liquid nitrogen, and stored as microsome stocks at −80°C until use.

Microsome stocks were thawed, pelleted at 436,000 *g* for 15 min at 2°C, and resuspended by pipetting in a buffer containing 10 mM Hepes, pH 7.2, 110 mM KCl, 10 mM NaCl, 1 mM $MgCl_2$, 5 mM KH_2PO_4, 1 mM DTT, 0.1 mM PMSF, 10 μM leupeptin, 1 μM pepstatin A, and 200 nM free calcium buffered in Ca-EGTA (Tsien and Pozzan, 1989). The microsome fraction was adjusted to a final concentration of 1 mg protein per ml. ^{45}Ca (DuPont-New England Nuclear, Wilmington, DE) was then added at the concentration of 8 or 24 μCi/ml. Calcium uptake was initiated by adding 2 mM ATP and allowed to saturate for >20 min at 20°C. Heparin, an $InsP_3$ receptor antagonist, was added 20 min after ATP addition. Addition of $InsP_3$ was followed by spotting a 20-μl aliquot of the solution onto a 0.45-μm filter (Type HA; Nihon Millipore, Tokyo, Japan). The filters were dried thoroughly, soaked in 6 ml of AQUASOL-2 (DuPont-New England Nuclear), and assayed by scintillation counting. The amount of released calcium was calculated by subtracting the radioactivity in the presence of $InsP_3$ from that in the absence of the $InsP_3$ and presented as the percentage of the calcium taken up into the microsomes.

Results

Calcium Waves Associated with Cleavage Furrows

The spatio-temporal patterns of calcium waves associated with cleavage furrows were characterized by confocal microscopy. Fertilized eggs were injected with 20 nl of 0.375 or 0.5 mM Calcium Green-1 and observed from the vegetal side with an inverted microscope, as the animal hemi-

1. *Abbreviations used in this paper*: CaGDx, dextran-conjugated Calcium Green-1; IICR, $InsP_3$-induced calcium release; $InsP_3$, inositol 1,4,5-trisphosphate; RhBDx, dextran-conjugated rhodamine B; ROI, region of interest.

spheres of *Xenopus* eggs, which are oriented upward, are heavily pigmented. The first and second cleavages of *Xenopus* eggs initiate at the animal pole, and the cleavage furrows progress toward the vegetal pole. After apparent completion of first cleavage, free calcium rose locally at the cleavage furrows (15/15 eggs from five females, in 0.02× Steinberg's solution; all embryos developed at least until blastula stage). An example from an embryo that grew to tadpole stage after the measurement is shown in Fig. 1. First cleavage formation had apparently completed at time point 0′. A calcium transient was observed at the first cleavage furrow during 2.3–8.3′ (Fig. 1 *A*). In this egg, free calcium rose at the vegetal side in one blastomere and traveled along the cleavage furrow as calcium waves. In the opposite blastomere, calcium waves were also observed (*4.3–6.3′* in Fig. 1 *A*). Thus, the pattern of free calcium elevation was not always symmetrical with respect to the cleavage furrows. The rise of free calcium subsided (*10.3′* in Fig. 1 *A*) and occurred again when the second cleavage was progressing (*20.3′* in Fig. 1 *A*). The second cleavage formation was also followed by calcium transients localized at second cleavage furrows (*30.3–36.3′* in Fig. 1 *A*). Fig. 1 *B* shows the apparent morphological change after the calcium transient at the first cleavage furrow. The newly formed blastomeres were separated from each other by a broad and obvious groove (*0.3′* in Fig. 1 *B*), which became obliterated (*10.3′* in Fig. 1 *B*) or "zipped" after localized calcium transients along the cleavage furrow had occurred (*4.3′* in Fig. 1 *B*). The maximum increase in fluorescence intensity (averaged over a region just beside the first cleavage furrow with the size of 0.5% area of the cell) was 1.64 ± 0.20-fold (mean ± SD, $n = 15$) compared with the value just before the calcium transient.

The detailed spatio-temporal pattern varied among eggs even taken from the same female. In some cases, the calcium waves originated at the animal side of the embryo

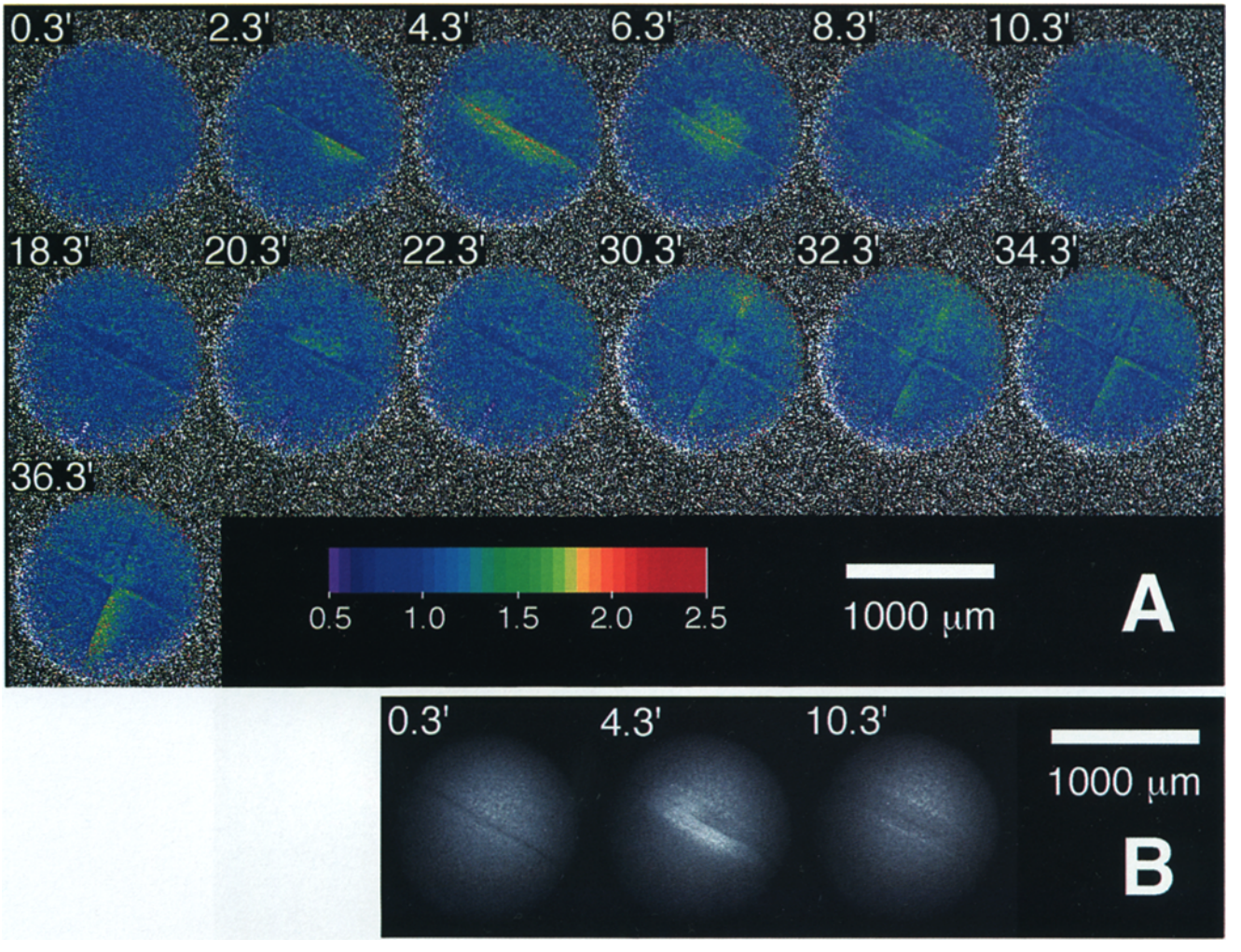

Figure 1. Calcium waves follow cleavage furrow formation. Fertilized eggs were injected with Calcium Green-1 and were observed after the onset of the first cleavage with a confocal laser-scanning microscope equipped with a Nikon ×4/0.13 NA objective lens. The timing at the apparent completion of the first cleavage furrow is defined as time 0 min (designated as 0′). Observations were carried out in 0.02× Steinberg's solution at 25°C. The embryo shown here developed to a normal tadpole after measurement. (*A*) Time-lapse images divided (pixel-by-pixel) by the image at 0′. The changes in fluorescence intensity are presented in pseudo-color (1.0-fold as *blue*, 2.5-fold as *red*). The calcium signal appeared in the range of green to yellow. The red spots in the image 4.3′ and 6.3′ are artifacts due to a slight move of the furrow (see the image at *4.3′* in *B*). (*B*) Calcium Green-1 fluorescence images of the same egg as in *A*.

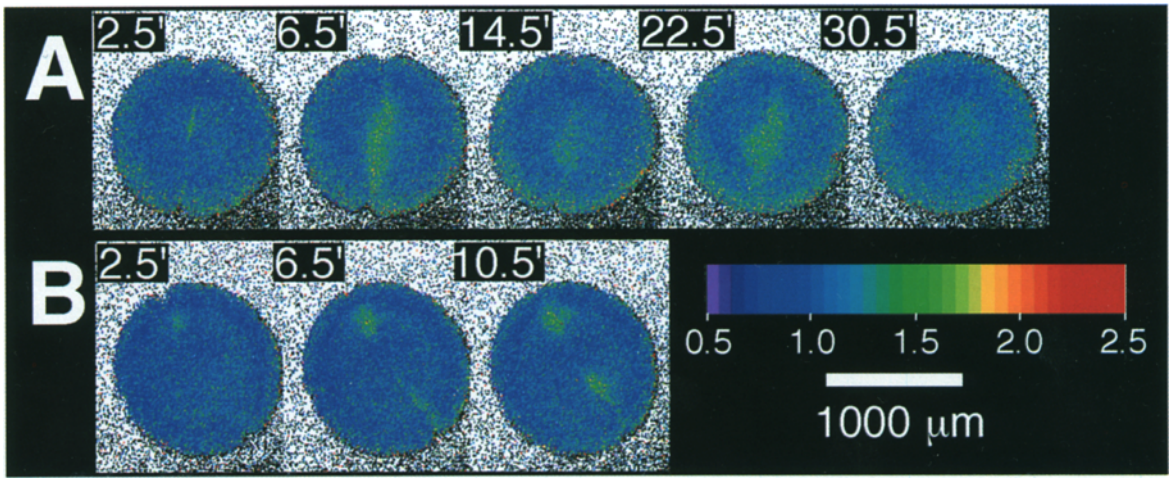

Figure 2. Calcium waves at the cleavage furrows demonstrated by ratiometric imaging (CaGDx/RhBDx). Fertilized eggs were coinjected with dextran-conjugated Calcium Green-1 and dextran-conjugated rhodamine B. Calcium Green-1 fluorescence images were divided pixel-by-pixel with rhodamine B fluorescence images. The ratio (CaGDx/RhBDx) in the image at time 0′ was adjusted to 1.0. The changes in fluorescence intensity are shown in pseudo-color (1.0-fold as *blue*, 2.5-fold as *red*). (*A*) Calcium waves along the first cleavage furrow. The measurement was started at time 0′, just after the first cleavage furrow formation. Calcium rises were observed twice (at *6.5′* and at *22.5′*). At 22.5′, the second cleavage came to the equatorial region. (*B*) Calcium waves after the second cleavage furrow formation. The measurement was started at time 0′, when the second cleavage was progressing at the equatorial region.

and propagated towards the vegetal pole. In other cases, the calcium wave was initiated in the vegetal side and propagated along the cleavage furrow. Calcium waves at the cleavage furrows were observed in succeeding cleavages at least until blastula stage.

When the focal plane was set deep inside the vegetal hemisphere, ring-shaped images were obtained (data not shown), which implied that the light could not pass inside the egg. Thus, the fluorescence signals observed above reflect the calcium changes near the surface of the eggs.

Ratiometric Measurements Using Control Dye

In the present study, we mainly used dextran-free Calcium Green-1, which was favorable for the rapid diffusion in the large *Xenopus* eggs (1.1–1.2-mm-diam) within a limited time. The toxicity of this dye was low enough to follow the normal development of *Xenopus* embryos. However, the use of one-wavelength calcium indicator dye is subjected to several artifacts. To confirm that the fluorescence changes observed above reflect intracellular free calcium changes and not the uneven distribution of the dye or changes in the cortical permeability of the fluorescence, dextran-conjugated Calcium Green-1 (mol wt 10,000) (CaGDx) and dextran-conjugated rhodamine B (mol wt 10,000) (RhBDx) were coinjected into fertilized eggs. RhBDx was used as a control dye independent of calcium concentration. Rhodamine B and Texas red, which have been successfully used as control dyes in other species (McDougall and Sardet, 1995; Stricker, 1995), inhibited

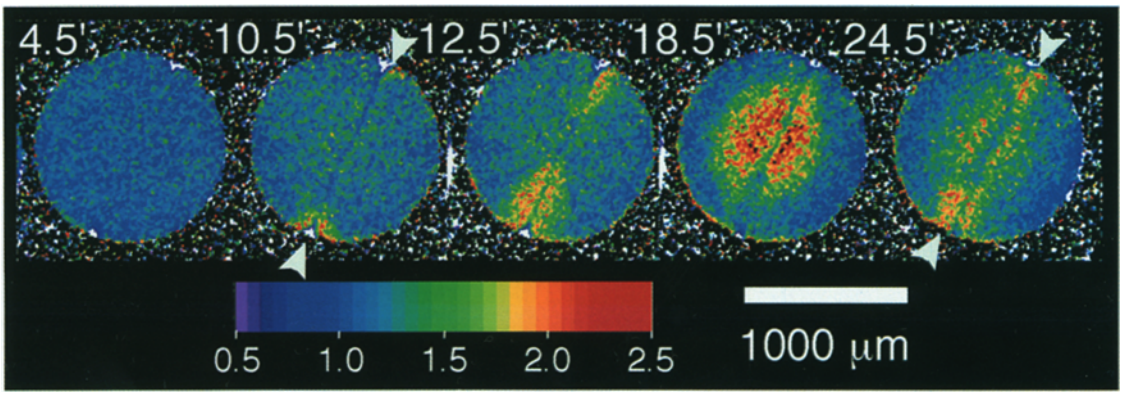

Figure 3. Calcium waves occur in the absence of extracellular calcium. Eggs were injected with Calcium Green-1 and were observed in 20 μM EGTA/distilled water at 26°C. The images were divided pixel-by-pixel with the image at 0′ when the first cleavage was formed in animal hemisphere. The changes in fluorescence intensity are shown in pseudo-color (1.0-fold as *blue*, 2.5-fold as *red*). The first cleavage formation was followed by calcium waves (*10.5′*; *arrowheads*). Note that the calcium waves occurred once again at 24.5′ (*arrowheads*) when the second cleavage furrow was extending to the equatorial region (not apparent in this vegetal view). The wave velocity was estimated as 2.8 μm/s in this egg.

cleavage furrow extension in *Xenopus* embryos in the laser-illuminated region in a dose-dependent manner (data not shown). For this reason, observations were started just before the calcium transients were expected to occur. In Fig. 2, ratio images (CaGDx/RhBDx) are shown, in which the CaGDx images were divided pixel-by-pixel with RhBDx images. Starting the laser scanning just after the first cleavage formation had apparently completed (time 0′), calcium transients were observed to appear twice at the first cleavage furrow (*6.5′* and *22.5′* in Fig. 2 *A*). The calcium waves after the second cleavage furrow formation were also observed (Fig. 2 *B*) on the condition that the laser scanning began after the second cleavage furrow had extended to the equatorial region (time 0′). Thus, the spatio-temporal pattern of calcium mobilization was similar to that obtained using Calcium Green-1 alone.

These results support the view that the localized changes in Calcium Green-1 fluorescence intensity (Fig. 1) reflected the intracellular free calcium changes and were not artifacts due to the concentration changes of the dye itself at cleavage furrows or the changes in the permeability of the light at the cortical surface.

Calcium Waves Occur without Extracellular Calcium

To determine if the extracellular calcium participates in the formation of calcium waves, measurements were performed against eggs placed in distilled water containing EGTA. Although embryos grown in the calcium-free solution died of lysis after several cell divisions, calcium waves were always observed after the first and second cleavage furrow formations (17/17 eggs from nine females). An example is shown in Fig. 3 in which the egg was placed in 20 μM EGTA/distilled water. Calcium waves were observed to accompany the first cleavage furrow formation (*10.5′–18.5′* in Fig. 3). In this egg, the calcium waves propagated from the animal side towards the vegetal pole from both ends of the furrow (*arrowheads* at *10.5′* in Fig. 3) and combined as they reached the vegetal pole (*18.5′* in Fig. 3), and then almost ceased (*24.5′* in Fig. 3). Calcium waves occurred once again at the first cleavage furrow (*arrowheads* at *24.5′* in Fig. 3), while the second cleavage furrow was forming toward the equatorial region (not apparent in this vegetal view). Although, in the egg shown in Fig. 3, calcium waves came from the animal side, the calcium waves initiated from variable sites among eggs observed, which was similar to the results obtained in 0.02× Steinberg's solution. In some of the other eggs, calcium waves initiated in the vegetal hemisphere and propagated along the furrows. From those eggs in which calcium waves traveled from the animal side, the wave velocity was estimated to be 3.08 ± 0.93 μm/s (mean ± SD, $n = 6$). There was a tendency for calcium signals to be larger in the absence of extracellular calcium or in diluted Steinberg's solutions (compare Fig. 3 with Fig. 1 *A*; see also Fig. 4). Although the reason is unclear, assuming that the intracellular calcium concentration is lowered by the depletion of the extracellular calcium, this could be attributed in part to the apparent increase of F/F_0 (where F_0 is the fluorescence intensity before calcium mobilization).

These results demonstrate that the calcium waves along the cleavage furrows can be formed in the absence of extracellular calcium.

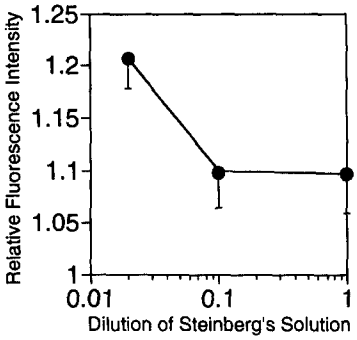

Figure 4. The extent of calcium mobilization is more prominent in diluted Steinberg's solution. The maximal changes in fluorescence intensity (changes in 5 min) averaged around the first cleavage furrow (20% area of the cell) were plotted as a function of dilution of Steinberg's solution. Mean ± SD (0.02×, $n = 4$; 0.1×, $n = 5$; 1×, $n = 7$). All of the data were taken from the embryos that developed to normal tadpoles after the measurements in each diluted Steinberg's solution.

The Effect of Extracellular Medium on Calcium Mobilization

Although the egg developed in 0.02–1× Steinberg's solution, the calcium waves were more prominent in 0.02× Steinberg's solution than those observed in 1× Steinberg's solution (340 μM Ca^{2+}). To show the extent of calcium mobilization, the maximum changes of averaged fluorescence over the region (20% area of the cell) taken around the first cleavage furrow were plotted as a function of dilution of the Steinberg's solution (Fig. 4). It may be that with more extracellular calcium, the embryos would require less calcium mobilization from internal calcium stores.

Calcium Waves at the First Cleavage Furrow Are Blocked by Heparin

Calcium waves along the cleavage furrow were likely to be mobilized from internal calcium stores, as they could occur in the absence of extracellular calcium. We therefore examined the properties of calcium release from the channels located on the internal calcium stores. Two families of calcium channels have been shown to be located on intracellular calcium stores: the $InsP_3$ receptor and the ryanodine receptor (for review see Furuichi et al., 1994). Ryanodine receptors have been shown to be absent in *Xenopus* eggs based on the ryanodine-binding assay (Parys et al., 1992) or Western blot analysis (Muto, A., unpublished results), while $InsP_3$ receptors are abundant in eggs (Kume et al., 1993). To examine the involvement of the $InsP_3$ receptor in the formation of calcium waves along the cleavage furrows, the effect of heparin, which was used as a competitive $InsP_3$ receptor blocker, was examined. The presence of heparin or de-N-sulfated heparin, a heparin analog used in control experiments, did not affect Calcium Green-1 fluorescence in various concentrations of free calcium (data not shown). Heparin (mol wt ~3,500; Sigma Chemical Co.) was coinjected with Calcium Green-1 into

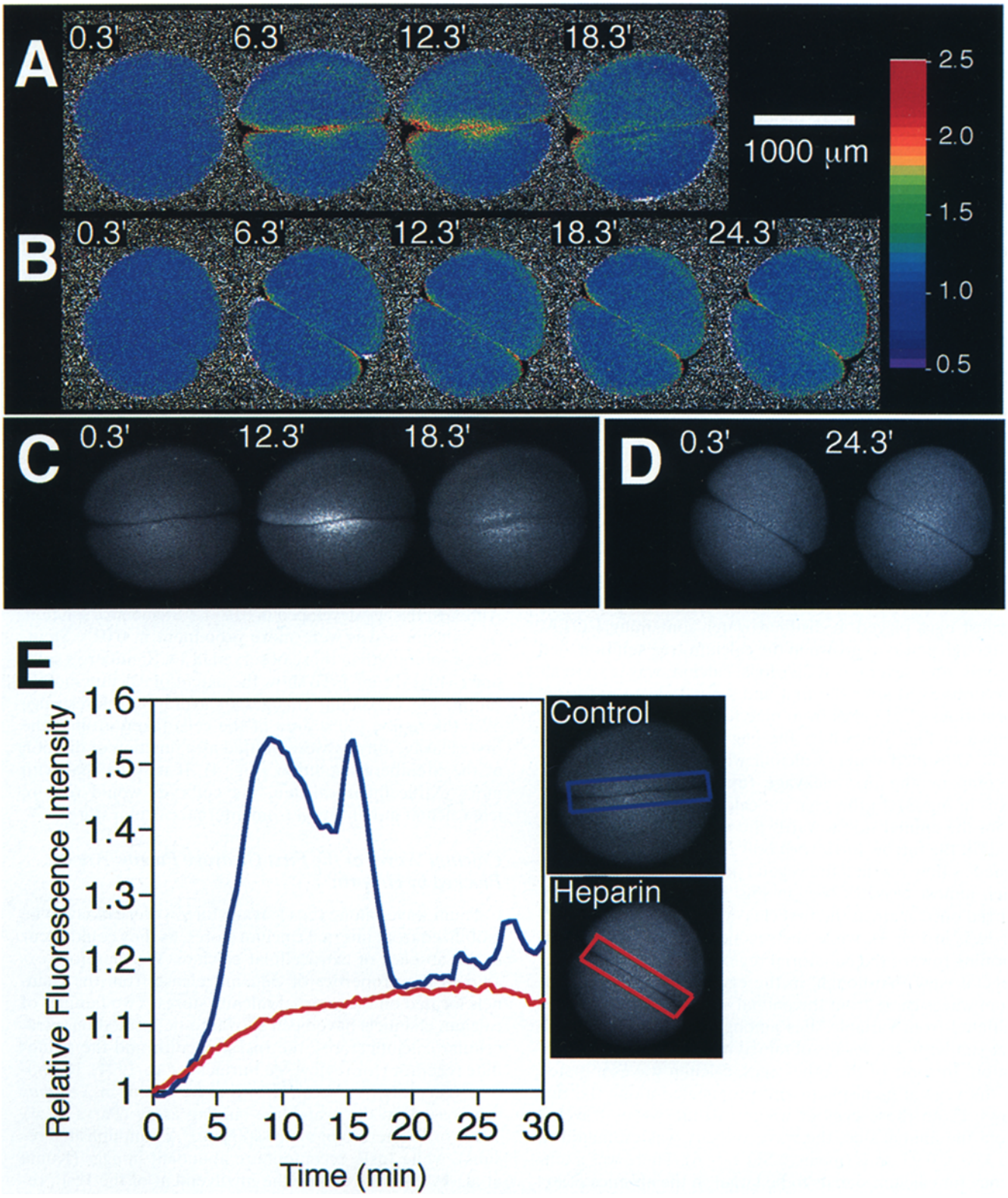

Figure 5. Heparin inhibits calcium waves at the first cleavage furrow. Heparin or de–N-sulfated heparin was coinjected with Calcium Green-1 into fertilized eggs. The fluorescence images were divided pixel-by-pixel with the image at 0′ when the first cleavage furrow formation had apparently been completed. The changes in fluorescence intensity are shown in pseudo-color (1-fold as *blue* and 2.5-fold as *red*). (*A*) Elevation of free calcium concentration was observed at the cleavage furrow in control embryo that was injected with de–N-sulfated heparin (final concentration: 90 μg/ml). (*B*) In the heparin-injected embryo, the free calcium elevation at the first cleavage furrow was inhibited. (*C*) Calcium Green-1 fluorescence images of the same egg in *A*. (*D*) Calcium Green-1 fluorescence images of the same egg in *B*. (*E*) Changes in fluorescence intensity averaged over the indicated region along the first cleavage furrow in the same embryos shown in *A* and *B*. (*Blue*) De–N-sulfated heparin (*Control*). (*Red*) Heparin. In the heparin-injected egg, the second cleavage furrow progressed to the equatorial region at 30 min but failed to complete.

fertilized eggs at 0.6–0.7 normalized time (fertilization at time 0, onset of first cleavage at time 1.0). The eggs were observed in 0.02 × Steinberg's solution. The free calcium elevation at the first cleavage was inhibited by heparin (estimated cytoplasmic concentration: 90 μg/ml; 7/8 eggs) (Fig. 5 *B*), whereas the control embryos injected with the same amount of de–N-sulfated heparin showed free calcium rises at the first cleavage furrows (6/6 eggs) (*6.3–12.3′* in Fig. 5 *A*). Typical examples are shown in Fig. 5. The apparent rise of fluorescence intensity at the edge of the blastomeres is an artifact that resulted from a slight change of shape, which did not change in time (Fig. 5, *C* and *D*). Average fluorescence changes over the first cleavage furrows in the eggs in Fig. 5, *A* and *B*, are shown in Fig. 5 *E*. No significant calcium transients occurred in the heparin-injected embryos, while sharp calcium transients were observed in control embryos. The second cleavage in heparin-injected embryos did not complete normally. Both the onset and the extension of the first cleavage furrow were retarded in heparin-injected embryos, and cell divisions thereafter were inhibited or greatly retarded, whereas eggs injected with de–N-sulfated heparin divided without significant retardation.

Similar to the results shown in Fig. 1 *B*, the zipping of the cleavage furrow can be observed in the control embryo. The first cleavage furrow in the control egg (*0.3′* in Fig. 5 *C*) appeared to be zipped (*18.3′* in Fig. 5 *C*) after the calcium rise (*12.3′* in Fig. 5 *C*) but not in the heparin-injected embryo (Fig. 5 *D*).

The dose-dependent effect of heparin is shown in Fig. 6. Maximal fluorescence changes averaged in small regions (0.5% area of the cell) beside the first cleavage furrow are indicated. More than 45 μg/ml of heparin showed an inhibitory effect on the calcium transients. Seven out of eight eggs that had been injected with 90 μg/ml heparin showed no calcium transients along the cleavage furrows.

These results demonstrate the involvement of $InsP_3$ receptor–mediated calcium release in the formation and propagation of calcium waves along the cleavage furrows.

Calcium Waves Localized to the Cleavage Furrows Are Distinct Events from Sinusoidal Calcium Oscillations with the Same Frequency as That of the Cell Division Cycle

Sinusoidal oscillation of intracellular calcium in cleavage-stage *Xenopus* embryos was characterized in its relation to calcium waves at the cleavage furrows. The sinusoidal calcium oscillation was originally measured by using a Ca^{2+}-sensitive microelectrode (Grandin and Charbonneau, 1991) or aequorin (Keating et al., 1994; Kubota et al., 1993). Since these observations did not reveal the spatial pattern of free calcium changes, it remained unclear whether the free calcium oscillation did not actually reflect the calcium waves at cytokinesis. Averaged fluorescence changes over the regions of interest (ROIs) during several cell division cycles were plotted in the same color of the ROIs (Fig. 7). This egg was observed in 1× Steinberg's solution. The fluorescence intensity averaged over the entire cell (Fig. 7, *inset*; ROI indicated in blue) showed a gradual, sinusoidal oscillatory change with a frequency similar to that of the cell division cycle (period: 25 min, plotted in blue), which

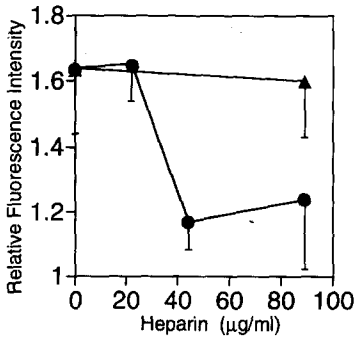

Figure 6. Dose-dependent effect of heparin on the localized calcium transients at the cleavage furrows. Heparin or de–N-sulfated heparin was coinjected with Calcium Green-1 into fertilized eggs. Maximal changes in Calcium Green-1 fluorescence intensity (changes in 5 min) averaged in small regions (0.5% area of the cell) beside the first cleavage furrows were plotted as a function of heparin concentration in the cells. Mean ± SD (heparin 0 μg/ml, $n = 15$; 22 μg/ml, $n = 6$; 45 μg/ml, $n = 4$; 90 μg/ml, $n = 8$; de–N-sulfated heparin 90 μg/ml, $n = 5$). (*Circle*) Heparin. (*Triangle*) De–N-sulfated heparin.

is referred to as calcium oscillation, as reported previously (Kubota et al., 1993). This calcium oscillation with the same period as the cell cycle (25 min) also emerged when the fluorescence intensity in the region not containing the first and second cleavage furrows (Fig. 7, *inset*; ROI indicated in red) was plotted (*red*). The calcium signals (*asterisks* at 20 and 40 min) in the small ROI (*green*; *inset*), derived from the localized calcium waves, appeared large, but its contribution to the gradual sinusoidal oscillation (*blue*) became decreased when divided by the entire area of the egg. This strongly suggests that the calcium oscillation over the entire region (*blue*) may not be mainly attributed to the calcium waves localized to the cleavage furrows (*green*). These observations were also confirmed by the fact that the intensity of the dye fluorescence also oscillated in cleavage-arrested eggs, which were coinjected with colchicine and Calcium Green-1 (data not shown). These observations were similar to the results showing that oscillation of chemiluminescence of injected aequorin persisted in cleavage-arrested eggs (Kubota et al., 1993). Gradual increase in the dye fluorescence during the observation (Fig. 7) was likely to reflect the increase in dye concentration at the vegetal side of the egg, for the diffusion of Calcium Green-1 did not reach a plateau even 3.5 h after the injection into *Xenopus* oocytes in which the intracellular free calcium concentration was considered to be constant (data not shown).

These results demonstrate that two types of calcium dynamics are present in cleavage-stage *Xenopus* embryos: one is the free calcium oscillation with the same frequency as that of the cell division cycle, which is distinct from the events at the cleavage furrows; the other is the localized calcium waves at the cleavage furrows.

$InsP_3$-induced Calcium Release from Microsomes and the Effect of Heparin

To confirm the presence of $InsP_3$-induced calcium release (IICR) and the effect of heparin on IICR during the cleav-

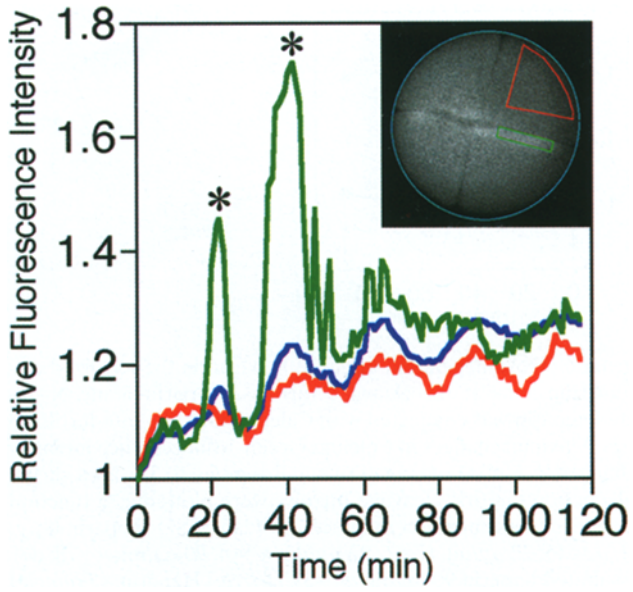

Figure 7. Periodic free calcium oscillation is distinct from the calcium waves at the cleavage furrows. Fertilized eggs were injected with Calcium Green-1 and observed in 1× Steinberg's solution. The averaged changes in intensity of Calcium Green-1 fluorescence over the ROIs indicated in the same colors were plotted. (*Blue*) Entire embryo. (*Red*) A region not containing first and second cleavage furrows. (*Green*) A region just beside the first cleavage furrow. The peaks indicated by asterisks (*green*) correspond to the calcium signals derived from the calcium waves (*inset*, in the ROI in *green*) along the cleavage furrow. Note that the fluorescence intensity averaged over the entire region (*blue*) shows gradual, sinusoidal oscillatory changes with the periodicity of the cell cycle (period: 25 min), referred to as calcium oscillation. These oscillatory changes are composed of two distinct components: one is calcium signals derived from calcium waves localized along the cleavage furrows (*green*), and the other is signals derived from calcium oscillation (period: 25 min; *red*) independent of calcium waves along the cleavage furrows.

age stage of *Xenopus*, IICR from embryo microsomes was characterized in vitro. Microsomes were prepared from 1–8-cell stage *Xenopus* embryos. Dose–response curves of calcium release by $InsP_3$ from microsomes of embryos are shown in Fig. 8 *A*. The ability of $InsP_3$ to release calcium was saturated at 200 nM in microsomes, and the 50% effective concentration (EC_{50}) of $InsP_3$ to release calcium was 20 nM. $InsP_3$ had a more potent calcium-releasing activity in the microsomes prepared from embryos than in those from oocytes (data not shown), suggesting that the calcium stores might be sensitized to $InsP_3$ during oocyte maturation or fertilization.

The effect of heparin on the calcium-releasing activity of microsomes prepared from *Xenopus* embryos was examined in vitro (Fig. 8 *B*). $InsP_3$ (100 nM)–induced calcium release was inhibited by 70% in the presence of 100 μg/ml heparin. De–N-sulfated heparin did not affect $InsP_3$-induced calcium release.

These results demonstrate the presence of IICR at the cleavage stage of *Xenopus*, which is inhibited by heparin in vitro.

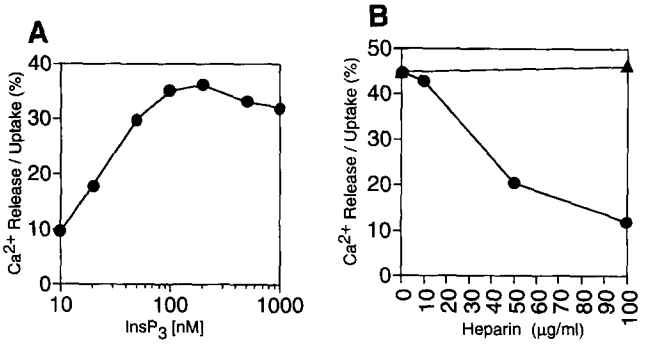

Figure 8. IICR from microsomes. (*A*) IICR from microsomes of *Xenopus* 1–8-cell embryos. The amounts of IICR are shown as a percentage of the calcium taken up into microsomes. Measurements were carried out at 25°C. (*B*) Inhibition of IICR ($InsP_3$; 100 nM) from 1–8-cell embryos by heparin. (*Circle*) Heparin. (*Triangle*) De–N-sulfated heparin.

Discussion

Calcium Dynamics in Xenopus Embryos

We have demonstrated that calcium waves occur along the cleavage furrows in *Xenopus* embryos. The calcium waves were observed to follow the preceding cleavage furrow formation. Furthermore, the calcium waves were observed not only in the vegetal side but also in the animal hemisphere using an upright microscope (data not shown), indicating that the calcium waves are not signals locally restricted to the vegetal side, but rather associated with the cleavage furrows in the whole embryo. Two types of calcium waves at cytokinesis were reported in medaka fish eggs: one followed the cleavage furrow extension, and the other with a larger amplitude was associated with subsequent apposition of the separating cell or zipping of the cleavage furrow (Fluck et al., 1991). In the present study, the cleavage furrow seemed to be zipped after calcium transients had occurred (see Figs. 1 *B* and Fig. 5, *C* and *D*), in a similar way to the observation of Fluck et al. (1991). Very recently, the calcium transient was shown to occur at the future cleavage furrow in zebra fish embryos (Chang and Meng, 1995), an event which had not been detected before in medaka fish eggs (Fluck et al., 1991). It remains to be elucidated if there are calcium transients preceding the cleavage furrow formation in *Xenopus* embryos.

We also showed that the sinusoidal calcium oscillation with the same frequency as that of the cell cycle (Grandin and Charbonneau, 1991; Keating et al., 1994; Kubota et al., 1993) was distinguishable from the calcium transients locally restricted to the cleavage furrows (Fig. 7). It is noticeable that periodic contractions of the cortex with the same period as the cell division cycle, visualized by time-lapse cinematography, persist even in cleavage-arrested *Xenopus* eggs (Hara et al., 1980). It is likely that the calcium oscillation observed here is closely related to the periodic surface contraction, although the biological significance remains uncertain at present.

Formation of Calcium Waves

Since the present results show that calcium waves along

the cleavage furrows are blocked by heparin, it seems likely that IICR is involved in this event. It has also been suggested that the calcium wave upon fertilization/egg activation in *Xenopus* eggs is mediated by the $InsP_3$ receptor (Nuccitelli et al., 1993). However, these two phenomena demonstrate very different characteristics. First, calcium waves along cleavage furrows are endogenously triggered by unknown mechanisms associated with the cell division cycle, whereas the calcium wave upon fertilization is triggered by a sperm that acts as an extracellular signal. Secondly, compared to the velocity of calcium waves at egg activation (9.7 μm/s at 22°C [Busa and Nuccitelli, 1985] or 8 μm/s at 22°C [Kubota et al., 1993]), the velocity of calcium waves along the cleavage furrows observed here was much slower (3.08 ± 0.93 μm/s at 25–26°C). Thirdly, the calcium waves in embryos are strictly restricted to the cleavage furrows, while the fertilization calcium wave travels the entire region in the egg. Considering these differences, it seems likely that there are different mechanisms for calcium wave propagation in egg activation and in cytokinesis of *Xenopus* eggs.

One possible mechanism for the localized calcium release along the cleavage furrows will be due to the localization of calcium stores at the cleavage furrows. Immunocytochemical study using an antibody raised against *Xenopus* type I $InsP_3$ receptor (Kume et al., 1993) has already indicated that $InsP_3$ receptors are not enriched at the cleavage furrow in *Xenopus* embryos (data not shown). At present, three types of $InsP_3$ receptors encoded by distinct genes have been identified in mammals (for review see Furuichi et al., 1994). Each subtype-specific mAb against human $InsP_3$ receptor (Sugiyama et al., 1994) recognized high molecular weight proteins in *Xenopus* embryos (Kume, S., unpublished results). Therefore, other subtypes of $InsP_3$ receptors possibly may be enriched along cleavage furrows and may be required for the formation of calcium waves. Another possible explanation is that activation of calcium release, such as $InsP_3$ production or $InsP_3$ receptor sensitization, is restricted to the cleavage furrows. The calcium changes in the eggs that failed to survive tended to be much larger and more extensive (e.g., egg in Fig. 3) than the eggs that developed normally (Fig. 1). This fact may imply that the calcium stores themselves are ubiquitously present all over the cell and, in abnormal conditions (e.g., no calcium outside the egg in the case of Fig. 3), the cells failed to keep the activation of calcium release moderate and restricted to the cleavage furrows.

Action of Mobilized Calcium

Very recently, it was shown that heparin (100 μg/ml) blocked the calcium transient at the future cleavage furrow and the cell division in zebra fish embryos (Chang and Meng, 1995). In *Xenopus* embryos, however, injection of heparin at a dose that inhibited calcium mobilization did not cause immediate arrest of cell cycle progression. The cell cycle was delayed, but the first cleavage occurred in embryos that were injected with 90 μg/ml heparin at 1-cell at 0.6–0.7 normalized time. The calcium transient at the first cleavage furrow was inhibited, but the second cleavage formation had started. The second cleavage could not complete normally in most cases. Taken together, calcium mobilization observed in this study is not likely to be essential in driving cell cycle progression. Although heparin has been shown to inhibit cell cycle progression (Chang and Meng, 1995; Ciapa et al., 1994; Han et al., 1992), it is difficult to specify the step of action of heparin in vivo. This is because $InsP_3$/calcium signaling seems to be involved in several steps in the cell cycle (Ciapa et al., 1994), such as nuclear membrane fusion demonstrated in *Xenopus* eggs in vitro (Sullivan et al., 1993).

Several possibilities could be raised about the physiological roles for mobilized calcium observed here. First, based on the observation of the morphological changes, zipping of the cleavage furrow, which is likely mediated by changes of cell adhesion molecules or the cytoskeleton, can be regulated by local calcium concentration. Secondly, mobilized calcium may promote the contraction of the contractile ring by activating one of the Ca^{2+}/calmodulin kinases, or myosin light chain kinase (Mabuchi and Takano-Ohmuro, 1990; Yamakita et al., 1994). Thirdly, the vesicle fusion, which was proposed as the mechanism to increase the membrane surface area accompanying cell division (Byers and Armstrong, 1986), may be regulated by calcium by a mechanism similar to exocytosis in membrane resealing (Bi et al., 1995).

Here we have demonstrated a close relationship between the calcium wave and cleavage furrow; however, the precise role of this calcium wave is obscure. The signaling mechanism leading to the mobilization of calcium and the target molecules of the mobilized calcium remain to be elucidated.

We thank Drs. Lee Sayers and Julie Matheson for a critical reading of the manuscript.

This work was supported by grants from the Ministry of Education, Science, and Culture of Japan (to S. Kume, H. Okano, and K. Mikoshiba), and research fellowships of the Japan Society for the Promotion of Science for Young Scientists (to S. Kume).

Received for publication 25 August 1995 and in revised form 9 July 1996.

References

Bi, G.-Q., J.M. Alderton, and R.A. Steinhardt. 1995. Calcium-regulated exocytosis is required for cell membrane resealing. *J. Cell Biol.* 131:1747–1758.

Busa, W.B., and R. Nuccitelli. 1985. An elevated free cytosolic Ca^{2+} wave follows fertilization in eggs of the frog, *Xenopus laevis*. *J. Cell Biol.* 100:1325–1329.

Byers, T.J., and P.B. Armstrong. 1986. Membrane protein redistribution during *Xenopus* first cleavage. *J. Cell Biol.* 102:2176–2184.

Cao, L.-G., and Y.-L. Wang. 1990. Mechanism of the formation of contractile ring in dividing cultured animal cells. II. Cortical movement of microinjected actin filaments. *J. Cell Biol.* 111:1905–1911.

Chang, D.C., and C. Meng. 1995. A localized elevation of cytosolic free calcium is associated with cytokinesis in the zebrafish embryo. *J. Cell Biol.* 131:1539–1545.

Ciapa, B., D. Pesando, M. Wilding, and M. Whitaker. 1994. Cell-cycle calcium transients driven by cyclic changes in inositol trisphosphate levels. *Nature (Lond.).* 368:875–878.

Fluck, R.A., A.L. Miller, and L.F. Jaffe. 1991. Slow calcium waves accompany cytokinesis in medaka fish eggs. *J. Cell Biol.* 115:1259–1265.

Furuichi, T., K. Kohda, A. Miyawaki, and K. Mikoshiba. 1994. Intracellular channels. *Curr. Opin. Neurobiol.* 4:294–303.

Grandin, N., and M. Charbonneau. 1991. Intracellular free calcium oscillates during cell division of *Xenopus Embryos*. *J. Cell Biol.* 112:711–718.

Han, J.-K., K. Fukami, and R. Nuccitelli. 1992. Reducing inositol lipid hydrolysis, $Ins(1,4,5)P_3$ receptor availability, or Ca^{2+} gradients lengthens the duration of the cell cycle in *Xenopus laevis* blastomeres. *J. Cell Biol.* 116:147–156.

Hara, K., P. Tydeman, and M. Kirschner. 1980. A cytoplasmic clock with the same period as the division cycle in *Xenopus* eggs. *Proc. Natl. Acad. Sci. USA.* 77:462–466.

Hepler, P.K. 1994. The role of calcium in cell division. *Cell Calcium.* 16:322–330.

Keating, T.J., R.J. Cork, and K.R. Robinson. 1994. Intracellular free calcium

oscillations in normal and cleavage-blocked embryos and artificially activated eggs of *Xenopus laevis*. *J. Cell Sci.* 107:2229–2237.

Kubota, H., Y. Yoshimoto, and Y. Hiramoto. 1993. Oscillation of intracellular free calcium in cleaving and cleavage-arrested embryos of *Xenopus laevis*. *Dev. Biol.* 160:512–518.

Kume, S., A. Muto, J. Aruga, T. Nakagawa, T. Michikawa, T. Furuichi, S. Nakade, H. Okano, and K. Mikoshiba. 1993. The Xenopus IP_3 receptor: structure, function, and localization in oocytes and eggs. *Cell.* 73:555–570.

Mabuchi, I., and H. Takano-Ohmuro. 1990. Effects of inhibitors of myosin light chain kinase and other protein kinases on the first cell division of sea urchin eggs. *Dev. Growth Differ.* 32:549–556.

McDougall, A., and C. Sardet. 1995. Function and characteristics of repetitive calcium waves associated with meiosis. *Curr. Biol.* 5:318–328.

Mittal, B., J.M. Sanger, and J.W. Sanger. 1987. Visualization of myosin in living cells. *J. Cell Biol.* 105:1753–1760.

Nuccitelli, R., D.L. Yim, and T. Smart. 1993. The Sperm-induced Ca^{2+} wave following fertilization of the Xenopus egg requires the production of $Ins(1,4,5)P_3$. *Dev. Biol.* 158:200–212.

Parys, J.B., S.W. Sernett, S. DeLisle, P.M. Snyder, M.J. Welsh, and K.P. Campbell. 1992. Isolation, characterization, and localization of the inositol 1,4,5-trisphosphate receptor protein in *Xenopus laevis* oocytes. *J. Biol. Chem.* 267: 18776–18782.

Poenie, M., J. Alderton, R.Y. Tsien, and R.A. Steinhardt. 1985. Changes of free calcium levels with stages of the cell division cycle. *Nature (Lond.).* 315:147–149.

Snow, P., and R. Nuccitelli. 1993. Calcium buffer injections delay cleavage in *Xenopus laevis* blastomeres. *J. Cell Biol.* 122:387–394.

Stricker, S.A. 1995. Time-lapse confocal imaging of calcium dynamics in starfish embryos. *Dev. Biol.* 170:496–518.

Sugiyama, T., A. Furuya, T. Monkawa, M. Yamamoto-Hino, S. Satoh, K. Ohmori, A. Miyawaki, N. Hanai, K. Mikoshiba, and M. Hasegawa. 1994. Monoclonal antibodies distinctively recognizing the subtypes of inositol 1,4,5-trisphosphate receptor: application to the studies on inflammatory cells. *FEBS Lett.* 354:149–154.

Sullivan, K.M.C., W.B. Busa, and K.L. Wilson. 1993. Calcium mobilization is required for nuclear vesicle fusion *in vitro*: implications for membrane traffic and IP_3 receptor function. *Cell.* 73:1411–1422.

Tombes, R.M., C. Simerly, G.G. Borisy, and G. Schatten. 1992. Meiosis, egg activation, and nuclear envelope breakdown are differentially reliant on Ca^{2+}, whereas germinal vesicle breakdown is Ca^{2+} independent in the mouse oocyte. *J. Cell Biol.* 117:799–811.

Tsien, R., and T. Pozzan. 1989. Measurement of cytosolic free Ca^{2+} with Quin-2. *In* Methods in Enzymology. Vol. 172. S. Fleischer and B. Fleischer, editors. Academic Press, Inc., San Diego, CA. 230–262.

Yamakita, Y., S. Yamashiro, and F. Matsumura. 1994. In vivo phosphorylation of regulatory light chain of myosin II during mitosis of cultured cells. *J. Cell Biol.* 124:129–137.

Yoshimoto, Y., T. Iwamatsu, and Y. Hiramoto. 1985. Cyclic changes in intracellular free calcium levels associated with cleavage cycles in echinoderm and medaka eggs. *Biomed. Res.* 6:387–394.